17th International Conference
ENGINEERING MECHANICS 2011
Svratka, Czech Republic, 9 – 12 May 2011

NANOINDENTATION BASED EVALUATION OF EFFECTIVE ELASTIC PROPERTIES OF METAL FOAM

V. Králík*, J. Němeček*

Abstract: *The paper aims to evaluate effective properties of a solid phase of metal foam on the level of a few microns. Basic principles of micromechanics are applied to the experimental results gained from nanoindentation. The paper describes microstructure and micromechanical properties of this highly porous material system. Results of elastic moduli were monitored in two distant locations on the metal foam pore walls. Elastic parameters were obtained on a statistical set of nanoindentation results from which one dominant and one minor mechanical phase were separated by the deconvolution algorithm. Effective elastic properties of a cell wall were evaluated by the Mori-Tanaka elastic homogenization.*

Keywords: ***Metal foam, porous system, nanoindentation, micromechanical properties, deconvolution.***

1. Introduction

Metal foams belong to the up-to-date structural materials with high potential to many engineering applications. This highly porous material with a cellular structure is known for its attractive mechanical and physical characteristics such as high stiffness in conjunction with very low weight, high strength, excellent impact energy absorption, high damping capacity and good sound absorption capability. The usual source material for the production of metal foams is aluminium and aluminium alloys because of low specific density (~2700 kg/m3), low melting point (~660 °C), nonflammability, possibility of recycling and excellent corrosion resistivity, (see e.g. the review by Banhart, 2001).

In general, mechanical properties of metal foams are governed by two major factors: (i) cell morphology (shape, size and distribution of cells) and (ii) material properties of the cell walls (Hasan et al., 2008). However, measurement of mechanical properties of the cell walls is a difficult problem that cannot be solved with conventional methods due to their small dimensions, low local bearing capacity and local yielding and bending of the cell walls. These problems can be overcome using micromechanical methods in which the load–displacement curve is obtained in the sub-micrometer range.

In this study, nanoindentation was applied to access elastic properties of the distinct phases within the cell walls. Based on these results, overall effective elastic properties of the solid phase were evaluated by micromechanical homogenization.

2. Materials and methods

2.1. Tested material

Commercial aluminium foam ‘Alporas’ (Shinko Wire Co., Ltd) was tested in this study. The manufacturing process of the Alporas is a batch casting process (Miyoshi et al., 1998). A typical resulting internal structure of the aluminium foam is shown in Fig. 1a.

Small Alporas block 18x18x14 mm was firstly embedded into cylindrical mould which was filled with a low viscosity epoxy resin (Struers®). Then, ~5 mm slice was cut by diamond saw and polished with fine SiC papers. Resulting surface roughness was checked with in-situ imaging (surface scanning was performed with the same tip as for nanoindentation). As a rule of thumb, the surface roughness should

* Ing. Vlastimil Králík and assoc. prof. Ing. Jiří Němeček, Ph.D.: Czech Technical Univerzity in Prague, Faculty of Civil Engineering, Department of Mechanics, Thákurova 2077/7; 166 29, Prague; CZ, e-mails: vlastimil.kralik@fsv.cvut.cz, jiri.nemecek@fsv.cvut.cz

be kept within 10% of the expected maximum depths used in nanoindentation. In our case, quadratic deviation from the mean plane (root-mean-square) was found to be $R_q \approx 9$ nm (according to ISO 4287:1997) which was acceptable compared to the maximum indentation depths 100 - 300 nm.

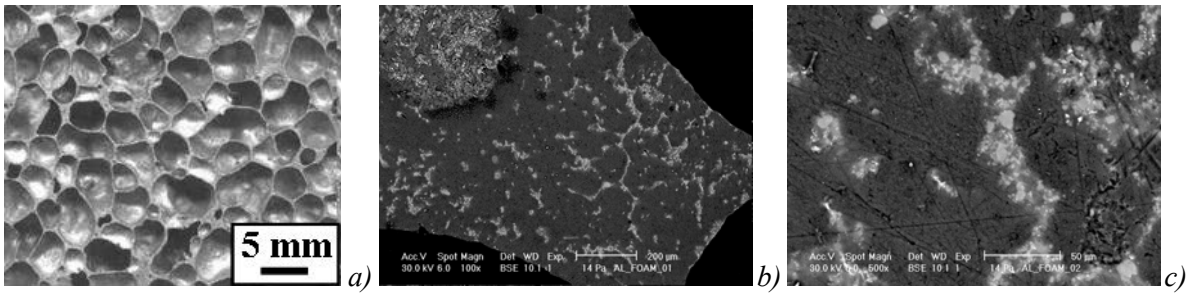

Fig. 1: a) Overall view on a typical structure of aluminium foam. b) ESEM image of a cell wall. c) Detailed ESEM image of a cell wall showing Ca/Ti-rich area (light zones).

The microstrucure of the foam was studied in electron microscope (ESEM). Two distinct phases, visible as differently colored areas in ESEM images were distinguished (Fig. 1b, c). The chemical composition of the two phases was checked with EDX element analysis in ESEM. As expected, the majority of the volume (dark zone) was composed of aluminum and aluminium oxide Al_2O_3 (further denoted as Al-rich area). Lighter zones contained significant amount of calcium and titanium (further denoted as Ca/Ti-rich area). The non-uniform distribution of these zones shows on inhomogeneous mixing of the admixtures that are added during the production process.

2.2. Nanoindentation

The nanoindentation testing was performed using a Hysitron Tribolab system® at the CTU in Prague. Two distant locations were chosen on the sample to capture its heterogeneity. Both locations were covered by a series of ~220 indents which was considered to give sufficiently large statistical set of data. Standard load controlled test of an individual loading diagram consisting of three segments: loading, holding at the peak and unloading was used. Loading and unloading of this trapezoidal loading function lasted for 5 seconds, the holding part lasted for 10 seconds. Maximum applied load was 1500 μN.

Elastic modulus was evaluated for individual indents using standard methodology (Oliver and Pharr, 1992) which accounts for elasto-plastic contact of a conical indenter with an isotropic half-space as:

$$E_r = \frac{1}{2\beta}\frac{\sqrt{\pi}}{\sqrt{A}}\frac{dP}{dh} \tag{1}$$

in which E_r is the reduced modulus measured in an experiment, A is the projected contact area of the indenter at the peak load, β is geometrical constant (β = 1.034 for the used Berkovich tip) and $\frac{dP}{dh}$ is a slope of the unloading branch evaluated at the peak. Elastic modulus E of the measured media can be found using contact mechanics which accounts for the effect of non-rigid indenter as:

$$\frac{1}{E_r} = \frac{\left(1-\nu^2\right)}{E} - \frac{\left(1-\nu_i^2\right)}{E_i} \tag{2}$$

in which ν is the Poisson's ratio of the tested material, E_i a ν_i are known elastic modulus and Poisson's ratio of the indenter. In our case, ν = 0.35 was taken as an estimate for all indents.

3. Results and discussion

3.1. Statistical and deconvolution results from nanoindentation

An example of a typical loading diagram gained from nanoindentation at Al-rich area (dark zone in Fig. 1b, c) is shown in Fig. 2a. Average contact depth is around 220 nm and maximum depth reaches values around 234 nm. Variety of results from different positions is shown on an example in Fig. 2b in which a pair of curves belongs to Al-rich and a pair to Ca/Ti-rich zones, respectively.

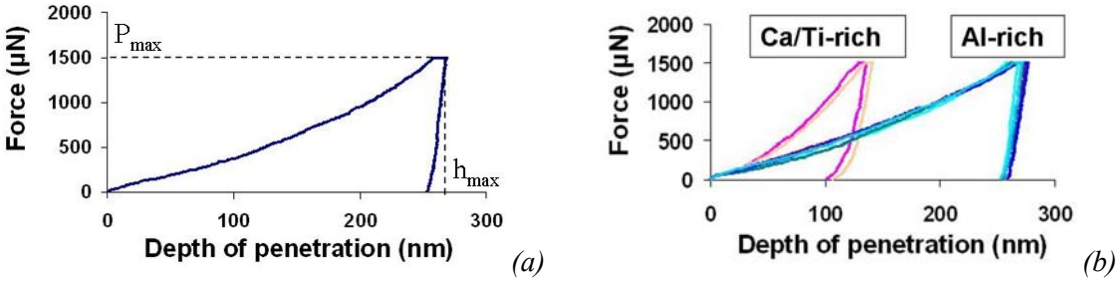

Fig. 2: (a) Typical loading diagram for Al-rich zone, (b) example of variation in loading diagrams for Al- and Ca/Ti-rich zones.

Elastic moduli were evaluated for each individual indent. Overall results are depicted in Fig. 3a in which histogram of all elastic moduli from two different positions and results merged from both positions are shown. No significant differences between the positions were found. Therefore, merged results were further used for the deconvolution of elastic properties. It can be seen in Fig. 3a that a significant peak appears around 60 GPa. This value can be considered as a dominant characteristic of a solid phase (Al-rich). The scatter in the results is affected mainly by the position in different zones (Al-rich, Ca/Ti-rich) and related hardnesses of its constituents in the sample.

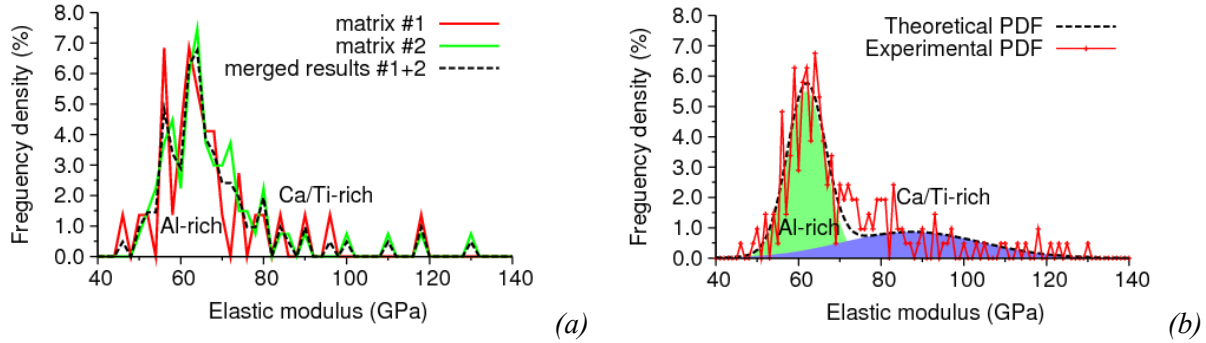

Fig. 3: (a) Probability density functions of elastic moduli from two measured positions and merged results. (b) Deconvolution of elastic moduli in two phases (Al-rich and Ca/Ti-rich).

Statistical results of elastic moduli (Fig. 3a) have been further analyzed with a deconvolution technique (Constantinides et al., 1998; Němeček et al., 2010; Němeček et al., 2011) which seeks for parameters of individual phases included in overall results. The deconvolution algorithm searches for n-Gauss distributions in an experimental probability density function - PDF (Fig. 3b). Random seed and minimizing criteria of the differences between the experimental and theoretical overall PDFs are computed in the algorithm to find the best fit. Two-phase system (one dominant Al-rich phase and one minor Ca/Ti-rich phase) was assumed in the deconvolution. Tab. 1 contains numerical results from the deconvolution with the estimated volume fractions of the phases.

Tab. 1: Elastic moduli and volume fractions from deconvolution.

Phase	***Mean (GPa)***	***St. dev. (GPa)***	***Volume fraction (-)***
1 (Al-rich zone)	*61.883*	*4.618*	*0.638*
2 (Ca/Ti-rich zone)	*87.395*	*16.684*	*0.362*

3.2. Effective material properties

Continuum micromechanics provides a framework, in which elastic properties of heterogeneous microscale phases are homogenized to give overall effective properties on the macroscale (Zaoui, 2002). In this context, representative volume element (RVE) is introduced in order to separate the scales. The RVE must be substantially smaller than the macroscale body, which allows imposing homogeneous boundary conditions over the RVE. This leads to constant stress/strain field in individual microscale components of ellipsoidal shapes. Effective elastic properties are then obtained through averaging over the local contributions. Considering isotropic spherical inclusions in a matrix leads to estimation of effective bulk modulus using so called Mori-Tanaka method as:

$$k_{\text{hom}} = \frac{\sum_r f_r k_r (1 + \alpha_0 (\frac{k_r}{k_0} - 1))^{-1}}{\sum_r f_r (1 + \alpha_0 (\frac{k_r}{k_0} - 1))^{-1}} \tag{3}$$

where f_r is the volume fraction of the r^{th} phase, k_r its bulk modulus and the coefficient α_0 describes bulk and shear properties of the 0^{th} phase, i.e. the reference medium (Zaoui, 2002).

The homogenized elastic properties for the two considered microscale phases were found to be $E_{hom} = 70.083$ GPa, $\nu_{\text{hom}} = 0.35$.

4. Conclusions

Performed microstructural observations and results from nanoindentation revealed that the heterogeneity included in the aluminium foam at the production process has consequences in its micromechanical behavior. Large scatter of elastic parameters have been obtained. Harder and softer areas measured with nanoindentation can be linked with ESEM analyses and denoted as Al- and Ca/Ti-rich areas. Statistical deconvolution was applied to find average elastic modulus of a dominant Al-rich phase (61.883 GPa) and minor Ca/Ti-rich phase (87.395 GPa). These microscale parameters together with their volume fractions were used in micromechanical up-scaling (Mori-Tanaka method) in which overall elastic properties for the homogenized medium (the whole metal foam wall) were found ($E_{hom} = 70.083$ GPa). It is planned to use the homogenized properties for further analysis of the macroscale behavior of the whole metal foam system including air pores.

Acknowledgement

Supports of the Czech Science Foundation (GAČR 103/09/1748) and Agency of the Czech Technical University in Prague, grant No. SGS10/135/OHK1/2T/11 are gratefully acknowledged.

References

Banhart J. (2001) Manufacture, characterisation and application of cellular metals and metal foams. Progress in Materials Science, 46, 6, pp.559-632.

Constantinides G., Chandran K.R., Ulm F.-J. & Vliet K.V. (2006) Grid indentation analysis of composite microstructure and mechanics: Principles of validation, Mat. Sci. and Eng., 430, 1-2, pp.189-202.

Hasan M.A., Kim A. & Lee H.-J. (2008) Measuring the cell wall mechanical properties of Al-alloy foams using the nanoindentation method, Composite Structures, 83, 2, pp.180-188.

ISO 4287:1997, "Geometrical Product Specifications (GPS) - Surface texture: Profile method".

Miyoshi T., Itoh M., Akiyama S. & Kitahara A. (1998) Aluminium foam, "ALPORAS": The production process, properties and application, Mat. Res. Soc. Symp. Proc., 521, pp.133-137.

Němeček J. & Lukeš J. (2010) On the evaluation of elastic properties from nanoindentation of heterogeneous systems, Chemické Listy, 104, pp.279-282.

Němeček J., Šmilauer V. & Kopecký L. (2011) Nanoindentation characteristics of alkali-activated aluminosilicate materials, Cement and Concrete Composites, 33, 2, pp.163-170.

Oliver W. & Pharr G. (1992) An improved technique for determining hardness and elastic modulus using load and displacement sensing indentation experiments, Journal of Material Research, 7, 6, pp.1564-1583.

Zaoui A. (2002) Continuum Micromechanics: Survey, Journal of Engineering Mechanics, 128, 8, pp.808-816.